J. Math. Computer Sci., 34 (2024), 217–233

Online: ISSN 2008-949X

Journal of Mathematics and Computer Science

Journal Homepage: www.isr-publications.com/jmcs

Haar wavelet based numerical technique for the solutions of fractional advection diffusion equations

Shahid Ahmed[a], Shah Jahan[a], Kottakkaran Sooppy Nisar[b,c,*]

[a]Department of Mathematics, Central University of Haryana, Mahendergarh-123029, India.

[b]Department of Mathematics, College of Sciences and Humanities in Alkharj, Prince Sattam Bin Abdulaziz University, Alkharj 11942, Saudi Arabia.

[c]Saveetha School of Engineering, SIMATS, Chennai, India.

Abstract

In this article, a new numerical technique based on Haar wavelet is introduced to solve the time fractional advection diffusion equations (TFADEs). First we have constructed a generalized operational matrix of fractional order integration using Haar wavelet without taking block pulse functions into account. The fractional derivative in these problems is in the Caputo sense. In the proposed technique, the unknown function is approximated by truncated Haar wavelet series. The efficiency of the computational approach is examined and validated using particular test problems, and are compared with those of existing methodologies. The numerical results show that the proposed technique is computationally more efficient and yields high accuracy over those methodologies. The behaviour of solutions of fractional order α and their graphical representation is shown by using MATLAB (R2022a) at various values.

Keywords: Advection diffusion equation, fractional calculus, Haar wavelet, multi-resolution analysis, error analysis.

2020 MSC: 35Q79, 65N35, 42C40, 26A33, 35R11.

1. Introduction

The calculus of fractions is an area of mathematics that investigates the characteristics of integrals and derivatives of orders that are not integers. It is the development of integer-order integrals and derivatives to real or even complex order. The complex-order derivative has allowed the order of fractional derivatives to be a function of independent variables like time, space, or other considerations. Fractional calculus has been one of the most useful and sophisticated techniques for expressing a wide range of physical processes over the last few decades [34], including gas transport through heterogeneous soil and gas reservoirs [6] and those in the fields of thermal sciences, viscoelasticity [4], electrochemistry, control theory [27], and traffic-flow simulation [5]. Non-locality is one of the most important characteristics of fractional-order models, which allows them to represent genuine physical phenomena and dynamic systems more precisely than standard differential operators. Much study has been conducted in the application of fractional calculus to many mathematical models that originate in the disciplines of engineering and science

*Corresponding author

Email addresses: shahjahan@cuh.ac.in (Shah Jahan), n.sooppy@psau.edu.sa (Kottakkaran Sooppy Nisar)

doi: 10.22436/jmcs.034.03.02

Received: 2023-07-21 *Revised:* 2023-12-16 *Accepted:* 2024-02-08

[1, 33]. It provides significant new capabilities for scientists, opening up new avenues for their work and making their discoveries applicable to a wide range of physical applications. The primary advantage of fractional calculus is that they are global operators that generate precise and stable results. For more information, see [24, 32]. Different hydrologic dynamics have been interpreted using fractional-derivative models, such as gas movement via heterogeneous soil and gas reservoirs [6]. Dissolved contaminants transport in groundwater [16]. Utilizing control system analysis in eye movement neurophysiology [27]. Numerous real-world phenomena that emerge in science and engineering could be the result of the construction of models based on the notion of fractional calculus. Some of these are the convection advection equation, the time fractional convection-diffusion equation, the time-fractional heat equations, the time fractional wave equation, the fractional Burger's equation, the fractional order Fisher's equation, and so on. Solving such fractional differential equations is challenging, so numerical methods play a crucial role. For the applications of fractional mathematical modeling, one can see [12, 20, 22, 23, 25, 26]. As a consequence, different numerical and analytical approaches have been effectively utilized to solve the fractional order equations. The fractional partial differential equations (FPDEs) are categorized as time-fractional partial differential equations (TFPDEs) and space-fractional partial differential equations. In this article, we'll concentrate on the TFPDEs, which are advection-diffusion equations with constant and variable coefficients,

$$\frac{\partial^{\alpha}\mu(\zeta,\tau)}{\partial\tau^{\alpha}}+a(\zeta)\frac{\partial\mu(\zeta,\tau)}{\partial\zeta}+b(\zeta)\frac{\partial^{2}\mu(\zeta,\tau)}{\partial\zeta^{2}}=R(\zeta,\tau),\quad 0<\zeta<1,\quad 0<\tau\leqslant 1, \tag{1.1}$$

with initial condition (IC)

$$\mu(\zeta,0)=f(\zeta),$$

and boundary conditions (BCs)

$$\mu(0,\tau)=h_0(\tau),\quad \mu(1,\tau)=h_1(\tau),$$

where $0<\alpha<1$ and $a(\zeta)$, $b(\zeta)\neq 0$ are continuous functions $f(.), h_0(.), h_1(\cdot)$ are functions in $L^2[0,1)$ and $h(.,.)$ is a given function in $L^2([0,1)\times[0,1))$. The Caputo fractional derivatives are used in this context to define the time-fractional derivative. Numerous numerical strategies have been developed for the solution since the analytic solution for FPDEs is challenging and requires more computational labor. FPDEs can be solved using a variety of numerical techniques, including the finite difference method, homotopy perturbation approach [21], generalized differential transform technique [24], Sinc-Legendre technique [28], discontinuous Galerkin technique [43], and variational iteration method [9]. Recently, several methods were proposed to develop the solutions of TFDEs, which include finite difference and finite volume schemes [14, 29], Gegenbauer spectral method [11], B-spline scaling function for time-fractional convection-diffusion equations [2], and high-order numerical algorithms for TFPDEs [46], Finite difference method for fractional dispersion equations [36], extended cubic B-spline technique [37], Chebyshev collocation methods [31, 35], and RBF-based local meshless method for fractional diffusion equations [13].

The popularity of wavelet-based numerical algorithms in numerical analysis may be attributed to their straightforwardness, computational simplicity, and speedy convergence. It's important to keep in mind that there are distinct wavelet families, including Chebyshev, Daubechies, Fibonacci, B-spline, Bernoulli, and Legendre wavelets, that are consistently used to solve various biological and physical problems [10, 17]. However, curiosity for the Haar wavelets has increased significantly, owing to their promising characteristics such as compact support, orthogonality, and lucidity [7]. Haar wavelets have more unique qualities that include their proficiency to recognize singular points, the simple incorporation of several forms of BCs, and the ability to integrate arbitrary times [32]. Currently, several researchers use numerical techniques based on wavelets to solve problems like TFPDEs. Particularly, Zada et al. [44] developed a numerical approach to solve FPDEs. A survey of different wavelet-based numerical methods has been found in [7]. For fractional PDEs, the Hermite wavelet was developed [10], and Jiaquan et al. used the Chebyshev wavelet for one-dimensional fractional convection diffusion equations [41, 42]. Chin et al. solved the fractional PDEs via wavelet techniques [8]. Wang solved the fractional Kadomtsov Petviashvili

Boney Moahony model [38] and the fractional Bogoyavlensky equation [39]. Further Wang gives a solitary wave solution to fractional KDV equations [40].

Motivated by Haar wavelet supremacy over other wavelet families, we set out to find a solution to the fractional-order equations by developing a modified Haar wavelet collocation fractional-order integration approach. Also, it is possible to implement the suggested approach by using the Walsh operational matrix of integration, regardless of the specific issue we are not going to discuss here, as the generalized Haar wavelet operational matrix of integration (OMI) is more viable and precise. The primary contribution of this study is, without applying the block pulse functions, OMIs of fractional order are constructed. Haar wavelets have the property of transforming the original equations into a series of algebraic equations with unknown coefficients. Apart from other approaches, ours does not involve computing the inverse of the Haar matrix. The significance of this work is to contribute to advancing numerical methods for solving TFADEs with improved efficiency and precision. The advantages of the considered problem are its relevance to real-world phenomena, and the advantages of the proposed techniques include versatility, computational efficiency, high accuracy, and a thorough comparative analysis with existing methodologies. Our results reveal that the present approach agrees perfectly with conventional techniques.

Sections are organized as follows. In Section 1, a brief introduction is discussed. Section 2 contains the basics of fractional derivatives and an overview of multi-resolution Haar wavelets and their function approximations. Further, the OMI of generalized Haar wavelets is constructed. In Section 3, the method of description of the proposed technique is obtained. In Section 4, the convergence and error analysis is given. In Section 5, four problems are discussed to demonstrate the effectiveness and accuracy of the current approach. Lastly, a brief conclusion was drawn.

2. Fractional calculus and Haar wavelet

In this part, we will first offer a quick introduction to certain requirements for fractional calculus before going into the Haar wavelets and their key characteristics. The Haar basis functions are used to construct fractional-order OMI.

2.1. Fractional calculus

Various techniques exist for defining fractional order derivatives, including Caputo, Riemann-Liouville (RL), Baleno fractional, and Grünwald-Letnikov. Since most physical processes begin with starting conditions specified in terms of field coordinates and their integer order, Caputo's method has proven to be remarkable [15, 32]. To avoid confusion, the fractional derivative will be used throughout the rest of this article in the sense of Caputo. For further studies, we refer to [32, 44].

Definition 2.1 ([15])**.** The RL fractional operator of order $\alpha > 0$ of $\mu(\zeta) \in \mathbb{C}_n, n > -1$ is

$$I^{\alpha}\mu(\zeta) = \frac{1}{\Gamma(\alpha)} \int_0^{\zeta} (\zeta - \tau)^{\alpha-1} \mu(\tau)\, d\tau, \quad \zeta > 0,$$

$\Gamma(.)$ denotes the gamma function. Few, properties of operator I^{α} are listed below:

1. $I^{\alpha} I^{\beta} \mu(\zeta) = I^{\alpha+\beta}\mu(\zeta),\ \alpha, \beta > 0;$
2. $I^{\alpha}\zeta^{\beta} = \dfrac{\Gamma(1+\beta)}{\Gamma(1+\alpha+\beta)}\zeta^{\alpha+\beta},\ \beta > -1;$
3. $I^{\alpha} I^{\beta} \mu(\zeta) = I^{\beta} I^{\alpha}\mu(\zeta),\ \alpha, \beta > 0.$

Definition 2.2. The Caputo fractional derivative D^{α} of $\mu(\zeta) \in \mathbb{C}_1^n$ is

$$D^{\alpha}\mu(\zeta) = \frac{1}{\Gamma(n-\alpha)} \int_0^{\zeta} \frac{\mu^n(\tau)}{(\zeta-\tau)^{\alpha-n+1}}\, d\tau, \quad n-1 < \alpha \leqslant n, \quad n \in \mathbb{N},$$

below are some fundamental features of the Caputo fractional derivative:

1. Linearity: $D^{\alpha}\big(\sigma\mu(\zeta)+\delta g(\zeta)\big)=\sigma D^{\alpha}\mu(\zeta)+\delta D^{\alpha}g(\zeta)$, where σ,δ are constants;
2. $I^{\alpha}D^{\alpha}\mu(\zeta)=\mu(\zeta)-\sum_{k=0}^{n-1}f^{k}(0^{+})\,\frac{\zeta^{k}}{k!}$, $n-1<\alpha\leqslant n$, $n\in\mathbb{N}$;
3. $D^{\alpha}\zeta^{\beta}=\dfrac{\Gamma(1+\beta)}{\Gamma(1+\beta-\alpha)}\,\zeta^{\beta-\alpha}$, $0<\alpha<\beta+1$, $\beta>-1$;
4. $D^{\alpha}C=0$, C is a constant.

2.2. Wavelets and multi-resolution analysis

A wavelet is a confined wave-like oscillation that develops from zero, achieves a maximum amplitude, and then declines back to zero amplitude. The earliest and most straightforward orthonormal wavelet with compact support among the several wavelet families that are now used is the Haar wavelet. The Haar wavelet family for $\zeta\in[0,1]$ can be computed as

$$h_i(\zeta)=\begin{cases}1, & \text{for } \zeta\in[\alpha,\beta),\\ -1, & \text{for } \zeta\in[\beta,\gamma),\\ 0, & \text{otherwise,}\end{cases}\tag{2.1}$$

where

$$\alpha=\frac{k}{m},\quad \beta=\frac{k+0.5}{m},\quad \gamma=\frac{k+1}{m}.$$

For $m=1,k=0$, we have $i=2$, is the minimal value and $N=2M=2^{j+1}$ is the maximal value. $i=1$ corresponding to the scaling function, i.e., $h_1(\zeta)=1$ in $[0,1]$, where m, $k\in\mathbb{Z}$, as $m=2^{j}, j=0,1,\ldots,J$, and J is the maximal level of resolution and the translation parameter is k, where $k=0,1,\ldots,m-1$. The index of h_i in (2.1) is given by $i=m+k+1$. For further studies on Haar wavelets and their applications one may see [17, 32]. Any $\mu\in L^{2}[0,1]$ can be transformed using Haar wavelet as

$$\mu(\zeta)=c_0h_0(\zeta)+c_1h_1(\zeta)+c_2h_2(\zeta)+\cdots=\sum_{i=0}^{\infty}c_ih_i(\zeta),$$

where c_i, $i=0,1,2,\ldots$ are the Haar coefficients given by

$$c_i=\langle\mu,h_i\rangle=\int_0^1\mu(\zeta)h_i(\zeta)\,d\zeta.$$

The preceding series terminate finitely if $\mu(\zeta)$ is piecewise constant throughout each subinterval or is piecewise constant consequently, the discrete matrix form is

$$\mu(\zeta)\approx\sum_{i=0}^{m-1}c_ih_i(\zeta)=C_m^{T}H_m,$$

where $C_m^{T}=[c_0,c_1,\ldots,c_{m-1}]$ are row vectors, and the Haar wavelet matrix H_m of order $m=2^{M}$. Collocation points are computed as

$$\zeta_l=\frac{l-0.5}{2M},\quad l=1,2,\ldots,2M.\tag{2.4}$$

The Haar matrix of order 8, i.e., $j=2\Rightarrow N=8$ is given as

$$H_8=\begin{pmatrix}1&1&1&1&1&1&1&1\\1&1&1&1&-1&-1&-1&-1\\1&1&-1&-1&0&0&0&0\\0&0&0&0&1&1&-1&-1\\1&-1&0&0&0&0&0&0\\0&0&1&-1&0&0&0&0\\0&0&0&0&1&-1&0&0\\0&0&0&0&0&0&1&-1\end{pmatrix}.$$

Integrating the Haar wavelet function one can obtain:

$$P_i(\zeta) = \int_0^\zeta h_i(\zeta')d\zeta', \qquad P_{i,1}(\zeta) = \begin{cases} \zeta - \alpha, & \text{for } \zeta \in [\alpha, \beta), \\ \gamma - \zeta, & \text{for } \zeta \in [\beta, \gamma), \\ 0, & \text{elsewhere.} \end{cases}$$

The next integral $Q_{i,2}(\zeta)$ of Haar wavelets may be determined in the following manner:

$$Q_{i,2}(\zeta) = \begin{cases} \frac{(\zeta-\alpha)^2}{2}, & \text{for } \zeta \in [\alpha, \beta), \\ \frac{1}{4m^2} - \frac{(\gamma-\zeta)^2}{2}, & \text{for } \zeta \in [\beta, \gamma), \\ \frac{1}{4m^2}, & \text{for } \zeta \in [\gamma, 1), \\ 0, & \text{elsewhere.} \end{cases}$$

Proceeding like this the n-th integration of Haar wavelets is

$$R_{i,n}(\zeta) = \begin{cases} \frac{(\zeta-\alpha)^n}{n!}, & \text{for } \zeta \in [\alpha, \beta), \\ \frac{(\zeta-\alpha)^n - 2(\zeta-\beta)^n}{n!}, & \text{for } \zeta \in [\beta, \gamma), \\ \frac{(\zeta-\alpha)^n - 2(\zeta-\beta)^n + (\zeta-\gamma)^n}{n!}, & \text{for } \zeta \in [\gamma, 1), \\ 0, & \text{elsewhere.} \end{cases}$$

Multi-resolution analysis: Multiresolution is intuitively connected to the study of signals or pictures with several degrees of resolution, similar to a pyramid. In the framework of wavelet analysis, Mallat and Meyer [19] proposed the concept of MRA in 1986.

Definition 2.3. A multi-resolution consists of a sequence $V_m : m \in \mathbb{Z}$ of embeded closed subspace of $L^2(\mathbb{R})$ satisfying the following:

- increasing, $V_m \subset V_{m+1} : m \in \mathbb{Z}$;
- density, $\bigcup_{m=-\infty}^{\infty}$ is dense in $L^2(\mathbb{R})$, i.e., $\overline{\bigcup_{m=-\infty}^{\infty} V_m} = L^2(\mathbb{R})$;
- separation, $\bigcap_{j\in\mathbb{Z}} V_m = 0$;
- scaling, $\mu(\zeta) \in V_m$, iff $\mu(2\zeta) \in V_{m+1}$, $\forall\ m \in \mathbb{Z}$;
- orthonormality, there exist $\phi \in V_0$ a scaling function such that $\phi_{o,k}(\zeta) = \phi(\zeta - k)$ is a basis for V_0.

By defining suitable projections of these functions onto these spaces, the space V_j may be utilized to approximate generic functions. Because the union of all V_0 is dense in $L^2(\mathbb{R})$, such projections can approximate any function in $L^2[\mathbb{R}]$ arbitrarily close.

2.3. Fractional operational matrix of integration

Here, integration of the vector $H_m(\zeta) = [h_0(\zeta), h_1(\zeta), \ldots, h_{m-1}(\zeta)]^T$ can be approximated by Haar series as [7]

$$\int_0^\zeta H_m(\eta)d\eta \cong PH_m(\zeta),$$

where P is the m order OMI. Next, the generalized OMI of general order is generated without using block pulse functions. The general order integration of the Haar operational matrix P^α is given by

$$P^\alpha H_m(\zeta) = I^\alpha H_m(\zeta) = \left[I^\alpha h_0(\zeta), I^\alpha h_1(\zeta), \ldots, I^\alpha h_{m-1}(\zeta)\right]^T = \left[Ph_0(\zeta), Ph_1(\zeta), \ldots, Ph_{m-1}(\zeta)\right]^T,$$

where

$$Ph_0(\zeta) = \frac{1}{\sqrt{m}}\,\frac{\zeta^\alpha}{\Gamma(1+\alpha)}, \quad 0 \leqslant \zeta \leqslant 1,$$

$$Ph_i(\zeta) = \frac{1}{\sqrt{m}}\begin{cases} 0, & 0 \leqslant \zeta < k-1/2^j, \\ 2^{j/2}\,\Phi_1(\zeta), & k-1/2^j \leqslant \zeta < k-0.5/2^j, \\ 2^{j/2}\,\Phi_2(\zeta), & k-0.5/2^j \leqslant \zeta < k/2^j, \\ 2^{j/2}\,\Phi_3(\zeta), & k/2^j \leqslant \zeta < 1. \end{cases}$$

$$\Phi_1(\zeta) = \frac{1}{\Gamma(\alpha+1)}\left(\zeta - \frac{k-1}{2^j}\right)^\alpha,$$

$$\Phi_2(\zeta) = \frac{1}{\Gamma(\alpha+1)}\left(\zeta - \frac{k-1}{2^j}\right)^\alpha - \frac{2}{\Gamma(\alpha+1)}\left(\zeta - \frac{k-0.5}{2^j}\right)^\alpha,$$

$$\Phi_3(\zeta) = \frac{1}{\Gamma(\alpha+1)}\left(\zeta - \frac{k-1}{2^j}\right)^\alpha - \frac{2}{\Gamma(\alpha+1)}\left(\zeta - \frac{k-0.5}{2^j}\right)^\alpha + \frac{1}{\Gamma(\alpha+1)}\left(\zeta - \frac{k}{2^j}\right)^\alpha.$$

For instance, if $\alpha = 1.5, N = 4$, and $N = 8$, we have

$$P^{1.5}H_4 = \begin{pmatrix} 0.0166 & 0.0864 & 0.1858 & 0.3079 \\ 0.0166 & 0.0864 & 0.1526 & 0.1351 \\ 0.0235 & 0.0751 & 0.0420 & 0.0319 \\ 0 & 0 & 0.0235 & 0.0751 \end{pmatrix},$$

$$P^{1.5}H_8 = \begin{pmatrix} 0.0042 & 0.0216 & 0.0465 & 0.0770 & 0.1122 & 0.1516 & 0.1948 & 0.2414 \\ 0.0042 & 0.0216 & 0.0465 & 0.0770 & 0.1039 & 0.1084 & 0.1019 & 0.0875 \\ 0.0059 & 0.0305 & 0.0540 & 0.0478 & 0.0331 & 0.0273 & 0.0238 & 0.0214 \\ 0 & 0 & 0 & 0 & 0.0059 & 0.0305 & 0.0540 & 0.0478 \\ 0.0083 & 0.0266 & 0.0149 & 0.0113 & 0.0095 & 0.0083 & 0.0075 & 0.0069 \\ 0 & 0 & 0.0083 & 0.0266 & 0.0149 & 0.0113 & 0.0095 & 0.0083 \\ 0 & 0 & 0 & 0 & 0.0083 & 0.0266 & 0.0149 & 0.0113 \\ 0 & 0 & 0 & 0 & 0 & 0 & 0.0083 & 0.0266 \end{pmatrix}.$$

3. Description of method

This part aims to demonstrate the applicability of the OMI of the generalized Haar wavelet for solving the TFPDEs with boundary conditions. Consider TFPDEs with variable coefficient

$$\frac{\partial^\alpha \mu(\zeta,\tau)}{\partial t^\alpha} + a(\zeta)\frac{\partial \mu(\zeta,\tau)}{\partial \zeta} + b(\zeta)\frac{\partial^2 \mu(\zeta,\tau)}{\partial \zeta^2} = R(\zeta,\tau), \quad 0 < \zeta < 1, \quad 0 < \tau \leqslant 1, \tag{3.1}$$

along with IC

$$\mu(\zeta,0) = f(\zeta), \quad 0 < \zeta < 1, \tag{3.2}$$

and BCs

$$\mu(0,\tau) = h_0(\tau), \qquad \mu(1,\tau) = h_1(\tau), \tag{3.3}$$

where $R(\zeta)$, $b(\zeta) \neq 0$, and $a(\zeta)$ are smooth functions, and $f(\zeta), h_0(\tau)$, and $h_1(\tau)$ are functions in $L^2[0,1)$. To solve time fractional equation (3.1), we assume

$$\frac{\partial^{2+\alpha}\mu(\zeta,\tau)}{\partial \zeta^2 \partial \tau^\alpha} \approx \Psi^T(\zeta) C \Psi(\tau), \tag{3.4}$$

where C is unknown Haar wavelet coefficient. Using R-L fractional integral of order α, we integrate (3.4) w.r.t to τ as given by

$$\frac{\partial^2 \mu(\zeta,\tau)}{\partial \zeta^2} \approx \left.\frac{\partial^2 \mu(\zeta,\tau)}{\partial \zeta^2}\right|_{\tau=0} + \Psi^T(\zeta) C P^\alpha \Psi(\tau), \tag{3.5}$$

where $P^{\alpha} = P^{\alpha}_{2^{k-1}M\times 2^{k-1}M}$, using initial condition (3.2), enable to put in (3.5),

$$\frac{\partial^2 \mu(\zeta,\tau)}{\partial \zeta^2} \approx f''(\zeta) + \Psi^T(\zeta) C P^{\alpha} \Psi(\tau). \tag{3.6}$$

By integrating (3.6) w.r.t ζ, twice, we get

$$\mu(\zeta,\tau) \approx \mu(0,\tau) + \zeta \frac{\partial \mu(\zeta,\tau)}{\partial \zeta}\Big|_{\zeta=0} - \zeta f'(0) + \left(P^2\Psi(\zeta)\right)^T C \left(P^{\alpha}\Psi(\tau)\right) + f(\zeta) - f(0). \tag{3.7}$$

Taking $\zeta = 1$ in (3.7) and employing the conditions given in (3.3), we get

$$\mu(1,\tau) \approx \mu(0,t) + \frac{\partial \mu\,(\zeta,\tau)}{\partial \zeta}\Big|_{x=0} - f'(0) + \left(P^2\Psi(1)\right)^T C \left(P^{\alpha}\Psi(\tau)\right) + f(1) - f(0). \tag{3.8}$$

Therefore, we get

$$\frac{\partial \mu(\zeta,\tau)}{\partial \zeta}\Big|_{\zeta=0} \approx -\left(P^2\Psi(1)\right)^T C \left(P^{\alpha}\Psi(\tau)\right) + f(0) + f'(0) - f(1) + h_1(\tau) - h_0(\tau) = S(\tau). \tag{3.9}$$

Substituting (3.9) in (3.7), we obtain

$$\mu(\zeta,\tau) \approx \mu(0,\tau) + \zeta S(\tau) + f(\zeta) - f(0) - \zeta f'(0) + \left(P^2\Psi(\zeta)\right)^T C \left(P^{\alpha}\Psi(\tau)\right). \tag{3.10}$$

By one time differentiation of (3.10) w.r.t τ we get,

$$\frac{\partial \mu(\zeta,\tau)}{\partial \zeta} \approx S(\tau) + f'(\zeta) - f'(0) + (P\Psi(\zeta))^T C \left(P^{\alpha}\Psi(\tau)\right). \tag{3.11}$$

Applying the Caputo fractional derivative w.r.t τ in (3.10), we obtin the following equation

$$\frac{\partial^{\alpha} \mu(\zeta,\tau)}{\partial \tau^{\alpha}} \approx \left(P^2\Psi(\zeta)\right)^T C\Psi(\tau) + \zeta D^{\alpha} S(\tau) + D^{\alpha} h_0(\tau), \tag{3.12}$$

where

$$D^{\alpha} S(\tau) = -\left(P^2\Psi(1)\right)^T C\Psi(\tau) + \frac{\partial^{\alpha}}{\partial \tau^{\alpha}} h_1(\tau) - \frac{\partial^{\alpha} h_0(\tau)}{\partial \tau^{\alpha}}, \quad D^{\alpha} h_0(\tau) = \frac{\partial^{\alpha} h_0(\tau)}{\partial \tau^{\alpha}}.$$

By inserting equations (3.8), (3.11), (3.12) in (3.1) and using the pre-defined collocation points given in (2.4), and replacing $\approx$ by $=$, we get the system of algebraic equation of the form given below:

$$\begin{aligned} &\left(P^2\Psi(\zeta)\right)^T C\Psi(\tau) + \beta D^{\alpha} R(\tau) + D^{\alpha} h_0(\tau) + a(\zeta)(R(\tau) + f'(\zeta) - f'(0) \\ &+ (P\Psi(\zeta))^T C \left(U^{\alpha}\Psi(\tau)\right) + b(\zeta)(f''(\zeta) + \Psi^T(\zeta) C P^{\alpha}\Psi(\tau)) = h(\zeta,\tau). \end{aligned} \tag{3.13}$$

We obtain the unidentified generalized Haar coefficient C in (3.13), solving the system of equations by using an iterative method such as the Newton method. Finally, by inserting C in (3.10), we obtain an approximate solution.

4. Error estimation

Assume that $\mu(\zeta)$ fulfills the requirements of the Lipschitz condition on $[0,1]$, $\exists\ K > 0$, such that

$$|\mu(\zeta_1) - \mu(\zeta_2)| \leqslant K|\zeta_1 - \zeta_2|,\ \forall\, \zeta_1, \zeta_2 \in [0,1],$$

where K is Lipschitz constant. Consequently, Haar approximation $\mu_m(\zeta)$ of $\mu(\zeta)$ is obtained as

$$\mu_m(\zeta) = \sum_{i=0}^{m-1} c_i h_i(\zeta), \quad m = 2^{q+1},\ q = 0, 1, \ldots, M.$$

Then corresponding error norm at m-th level can be obtained as

$$\|\mu\zeta) - \mu(\zeta_m)\| = \|\mu\zeta) - \sum_{i=0}^{m-1} c_i h_i(\zeta)\|_2 = \| \sum_{i=2^{q+1}}^{\infty} c_i h_i(\zeta)\|.$$

We are able to carry out an error analysis since the exact solution to the fractional-order differential equations is already known. Here, in the context of an upper limit, we deduce an inequality, demonstrating the convergence of Haar wavelet for fractional order PDEs.

Theorem 4.1 ([18]). *Suppose the Lipschitz condition for the function $\mu(\zeta,\tau)$ on $[0,1]$ are satisfied and $\mu_m(\zeta,\tau)$ are the Haar approximations of $\mu(\zeta)$, then the error norm is*

$$\left\|\mu(\zeta,\tau) - \mu_m(\zeta,\tau)\right\|_2 \leqslant \frac{K}{\sqrt{3}\, m^2},$$

where

$$\|\mu(\zeta,\tau)\|_E = \left(\int_0^1 \int_0^1 \mu^2(\zeta,\tau) d\zeta d\tau\right)^{\frac{1}{2}}.$$

Theorem 4.2 ([7]). *Assume that the k-th derivative exist and bounded on $[a,b]$ for any $M = 2^j$, $j = 0,1,2,3,\ldots,$ if μ_M and μ are the Haar solution and exact solution, respectively, then*

$$\|\mu - \mu_M\|_\infty \leqslant \mathcal{O}\left(\frac{1}{M}\right)^2 \quad as \quad j \to \infty.$$

The absolute error to observe the performance and accuracy of Haar wavelet is defined as

$$E_r = |\mu(\zeta,\tau) - \mu_k(\zeta,\tau)|,$$

the exact solution is denoted as $\mu(\zeta,\tau)$ and $\mu_k(\zeta,\tau)$ is the approximate solution. The maximum absolute error is

$$L_\infty = \max|\mu(\zeta,\tau) - \mu_k(\zeta,\tau)|.$$

5. Numerical examples

To show how the generalized Haar wavelet technique works, we have presented some numerical examples in this section. The results are tabulated and contrasted with those from earlier methodologies that were reported in the literature and the absolute error is measured.

Problem 5.1. Consider $a(\zeta) = \zeta$ and $b(\zeta) = -1$ and

$$R(\zeta,\tau) = \frac{\Gamma(1+2\alpha)}{\Gamma(1+\alpha)}\tau^\alpha\left(\zeta - \zeta^3\right) + \left(1+\tau^{2\alpha}\right)\left(7\zeta - 3\zeta^3\right).$$

Then equation (1.1) becomes

$$\frac{\partial^\alpha \mu(\zeta,\tau)}{\partial\tau^\alpha} + \zeta\frac{\partial\mu(\zeta,\tau)}{\partial\zeta} - \frac{\partial^2\mu(\zeta,\tau)}{\partial\zeta^2} = \frac{\Gamma(1+2\alpha)}{\Gamma(1+\alpha)}\tau^\alpha\left(\zeta - \zeta^3\right) + \left(1+\tau^{2\alpha}\right)\left(7\zeta - 3\zeta^3\right), \quad 0 < \zeta < 1, 0 < \tau < 1,$$

with IC

$$\mu(\zeta,0) = \zeta - \zeta^3,$$

and BCs are

$$\mu(0,\tau) = 0 = \mu(1,\tau).$$

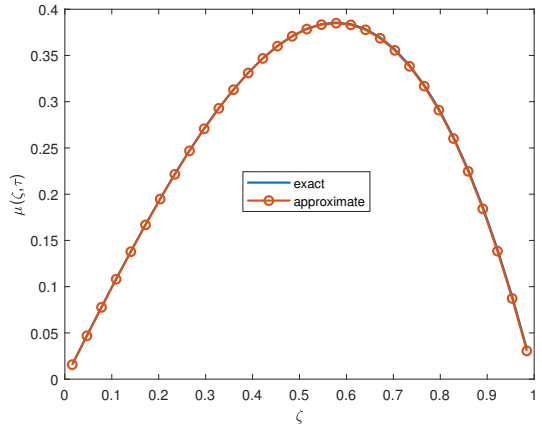

(a) Comparison of exact and approximate solution at j = 4.

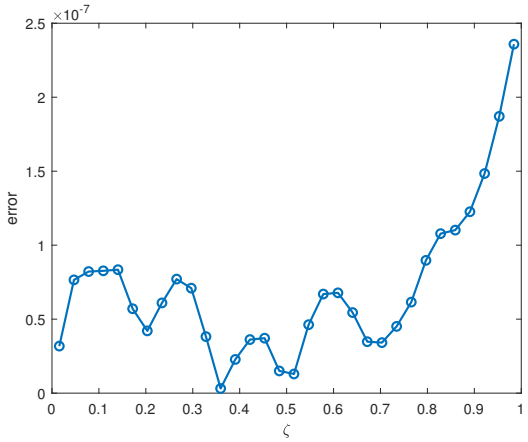

(b) Behaviour of absolute error at j = 4.

Figure 1: Plot of exact and approximate solutions for time $\tau = 0.1$ and $\alpha = 0.95$ of Problem 5.1.

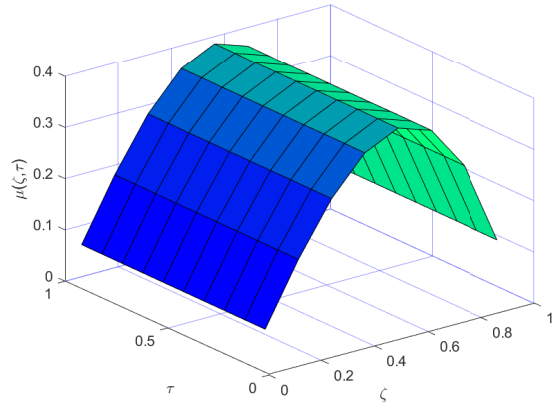

(a) Behaviour of approximate solutions at j = 3.

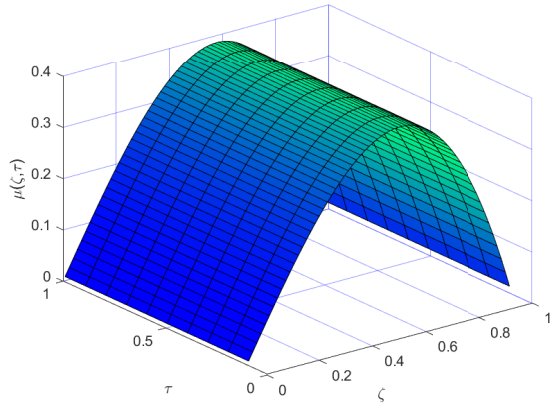

(b) Behaviour of approximate solutions at j = 4.

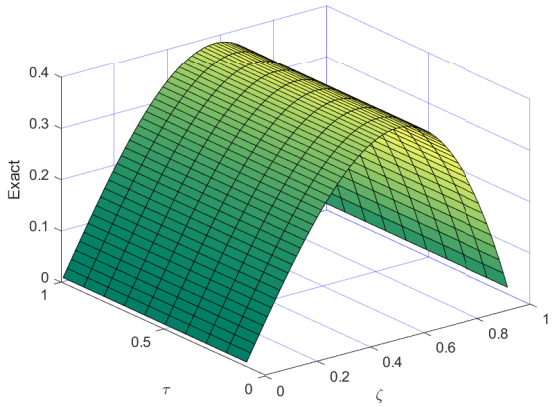

(c) Behaviour of exact solution at j = 4.

Figure 2: Graphs of approximate and exact solutions of Problem 5.1 at $\alpha = 0.95$.

Table 1: Absolute error of Problem 5.1 at various values of α and $\tau = 0.5$ with resolution $j = 4$.

ζ	α=0.1	α=0.3	α=0.5	α=0.7
0.1	3.4533e-05	2.4255e-05	8.1341e-05	1.2085e-06
0.2	4.6352e-05	2.4788e-05	1.7233e-05	7.6121e-05
0.3	5.3451e-05	6.0388e-05	1.4631e-04	1.5390e-05
0.4	6.2124e-05	6.6252e-05	8.6268e-04	3.4718e-05
0.5	7.0770e-05	1.2351e-05	5.5453e-04	1.9165e-06
0.6	8.5630e-05	4.7453e-05	1.2652e-04	1.0258e-05
0.7	9.7569e-05	5.3982e-05	2.2377e-05	6.1842e-05
0.8	1.0654e-04	6.0259e-05	2.2160e-05	6.5283e-06
0.9	1.3325e-04	9.2655e-05	3.4241e-05	9.2498e-06

Table 2: Absolute error of Problem 5.1 at $\alpha = 0.9$, $\tau = 0.1$ with resolution $j = 4$.

x	Chebyshev collocation method [31]		Present method	
	m=5	m=6	j=4	j=6
0.1	2.4568e-03	2.4473e-03	1.9579e-05	2.3215e-06
0.2	4.7198e-03	4.7146e-03	1.8181e-05	3.6568e-06
0.3	6.6174e-03	6.6114e-03	2.1976e-05	2.0309e-06
0.4	7.9816e-03	7.9728e-03	2.5772e-06	4.6186e-06
0.5	8.6666e-03	8.6566e-03	6.3649e-05	8.7586e-06
0.6	8.5616e-03	8.5537e-03	5.3649e-05	9.2855e-05
0.7	7.6045e-03	7.5997e-03	4.3685e-06	2.9346e-05
0.8	5.7951e-03	5.7900e-03	4.3685e-05	9.9165e-06
0.9	3.2082e-03	3.1971e-03	6.7125e-06	2.4445e-06

The given problem has an exact solution provided below as

$$\mu(\zeta,\tau) = \left(1+\tau^{2\alpha}\right)\left(\zeta-\zeta^3\right).$$

In Figures 1 and 2, approximate solutions and exact solutions are compared in two and three dimensions, and the behavior of approximate solutions at different resolution levels of the Haar wavelet is shown. Table 1 shows the absolute error at time $\tau = 0.5$ for different values of the fractional parameter α, and the comparison of the approximate solution with other methods is shown in Table 2.

Problem 5.2. Consider

$$\frac{\partial^\alpha \mu(\zeta,\tau)}{\partial \tau^\alpha} - \zeta\frac{\partial \mu(\zeta,\tau)}{\partial \zeta} - \frac{\partial^2 \mu(\zeta,\tau)}{\partial x^2} = R(x,\tau), \quad 0<\zeta<1, \quad 0<\tau\leqslant 1,\ 0<\alpha<1, \tag{5.1}$$
$$R(\zeta,\tau) = \frac{10\zeta^2(1-\zeta)\tau^{2-\alpha}}{\Gamma(2-\alpha)} - 10(\tau+1)\left(\frac{2}{\Gamma(1)} - \frac{6\zeta}{\Gamma(2)}\right) + 10(\tau+1)\left(\frac{2\zeta}{\Gamma(2)} - \frac{6\zeta^2}{\Gamma(2)}\right),$$

with IC

$$\mu(\zeta,0) = 10\zeta^2 - 10\zeta^3,$$

and BCs

$$\mu(0,\tau) = 0, \quad \mu(1,\tau) = 0.$$

The exact solution of (5.1) is

$$10(\tau+1)(1-\zeta)\zeta^2.$$

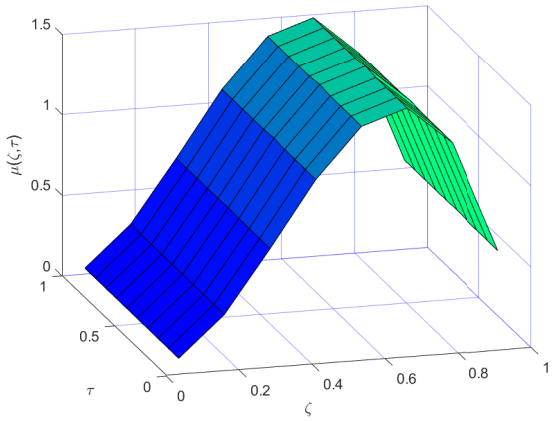

(a) Behaviour of approximate solutions at j = 3.

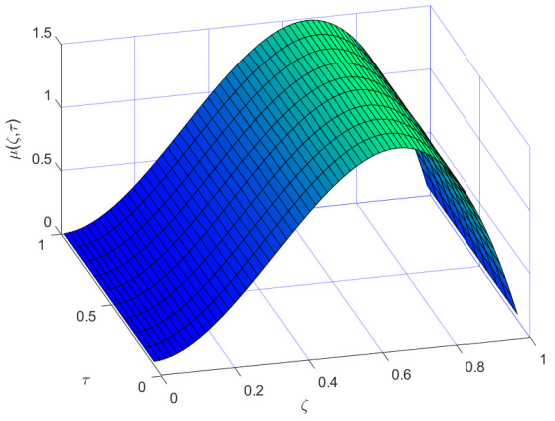

(b) Behaviour of approximate solutions at j = 4.

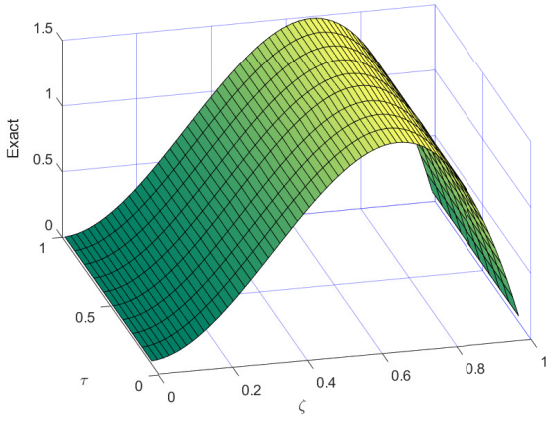

(c) Behaviour of exact solutions at j = 4.

Figure 3: Graphs of approximate and exact solution of Problem 5.2 at $\alpha = 0.05$.

Table 3: Absolute error of Problem 5.2 at different values of α and $\tau = 0.95$ with resolution j = 4.

ζ	α=0.01	α=0.03	α=0.05	α=0.07
0.1	5.3328e-04	2.4832e-03	8.1341e-04	1.2085e-03
0.2	2.5766e-04	2.4425e-04	1.7563e-04	7.6121e-03
0.3	3.1422e-04	6.0352e-04	1.4571e-04	1.5390e-04
0.4	4.5249e-04	6.6452e-03	8.6468e-03	3.4718e-04
0.5	2.7517e-04	1.2331e-04	5.5723e-04	0.0024
0.6	2.2554e-04	4.7243e-04	1.2482e-04	0.0027
0.7	1.2581e-04	5.3512e-04	0.0015	0.0029
0.8	2.9325e-04	0.0011	0.0019	6.5283e-03
0.9	3.5282e-04	0.0013	0.0023	0.0015

In Figure 3, the approximate solution and exact solution are compared in 3-dimensional, and the behavior of the approximate solution at various resolution levels of the Haar wavelet is also compared. Figure 4 represents the behavior of the approximate solution at different values of α. Table 3 shows the absolute error at time $\tau = 0.5$ for various values of the fractional parameter α, and a comparison of the approximate solution with existing techniques is given in Table 4.

Table 4: Absolute error of Problem 5.2 at different values of α and τ=0.95 with resolution $j = 4$.

ζ	Chebyshev wavelets[3]	Method in [45]	Present method
(0.1)	0.17775401	017760929	5.3327e-04
(0.2)	0.63545182	0.63439865	2.7514e-04
(0.3)	1.25138745	1.25076281	1.2581e-04
(0.4)	1.90954789	1.90718308	1.2585e-04
(0.5)	2.487001534	2.48418437	3.5282e-04
(0.6)	2.87001534	2.86234006	4.3875e-04
(0.7)	2.92456444	2.92227732	2.2551e-04
(0.8)	2.55014586	2.54468333	7.1839e-04
(0.9)	1.611254478	1.61031324	1.3528e-04

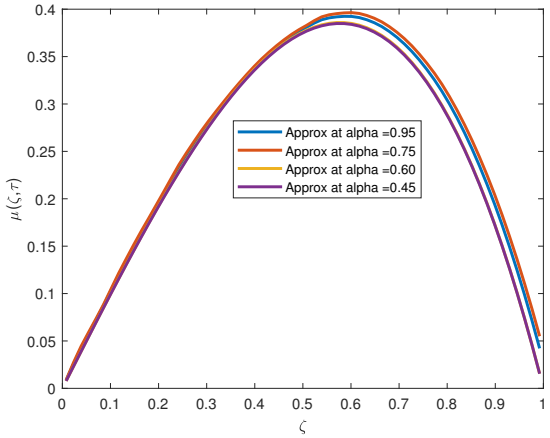

(a) Behaviour of approximate solutions at different values of α at $j = 4$ of Problem 5.1.

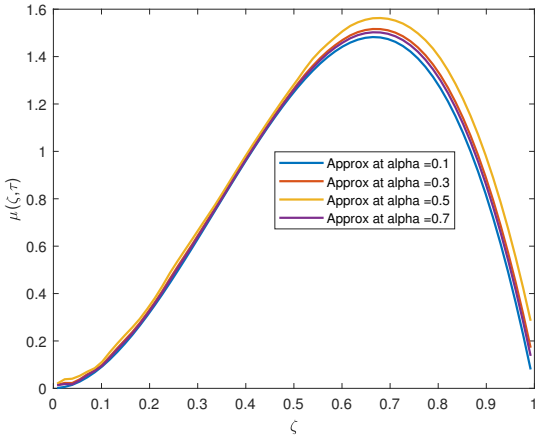

(b) Behaviour of approximate solutions at different values of α at $j = 4$ of Problem 5.2.

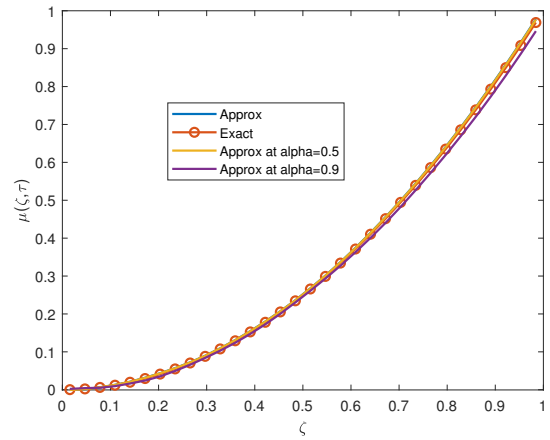

(c) Behaviour of approximate solutions at different values of α at $j = 4$ of Problem 5.3.

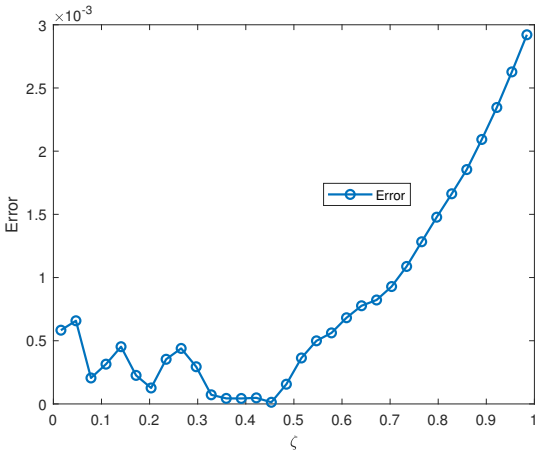

(d) Absolute error of Problem 5.2 at $\alpha = 0.05$.

Figure 4: Graphs of approximate solutions and absolute error.

Problem 5.3. Consider the following equation

$$\frac{\partial^{\alpha}\mu(\zeta,\tau)}{\partial\tau^{\alpha}} + \zeta\frac{\partial\mu(\zeta,\tau)}{\partial\zeta} + \frac{\partial^{2}\mu(\zeta,\tau)}{\partial\zeta^{2}} = 2\tau^{\alpha} + 2\zeta^{2} + 2, \quad 0 < \zeta < 1, \quad 0 < \tau \leqslant 1, \quad 0 < \alpha < 1,$$

with IC and BCs

$$\mu(\zeta,0)=\beta^2, 0<\zeta<1, \quad \mu(0,\tau)=\frac{2\Gamma(\alpha+1)}{\Gamma(2\alpha+1)}\tau^{2\alpha}, \quad \mu(1,\tau)=1+\frac{2\Gamma(\alpha+1)}{\Gamma(2\alpha+1)}\tau^{2\alpha}, 0\leqslant\tau\leqslant 1.$$

The given problem has an exact solution provided below:

$$\mu(\zeta,\tau)=\zeta^2+\frac{2\Gamma(\alpha+1)}{\Gamma(2\alpha+1)}\zeta^{2\alpha}.$$

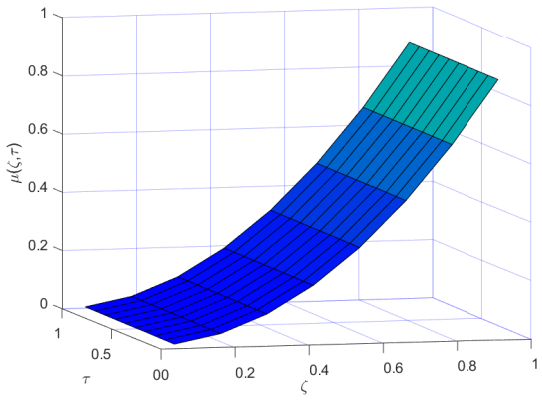

(a) Approximate solutions at j = 3.

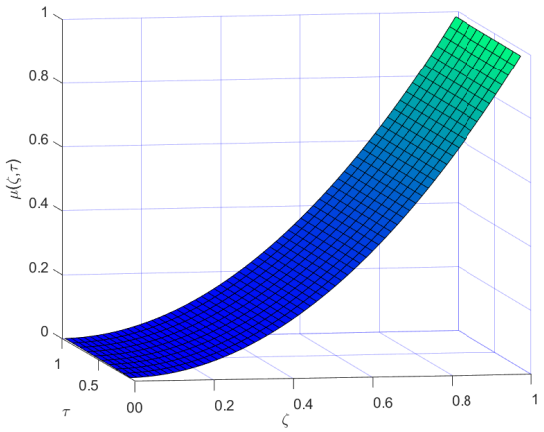

(b) Approximate solutions at j = 4.

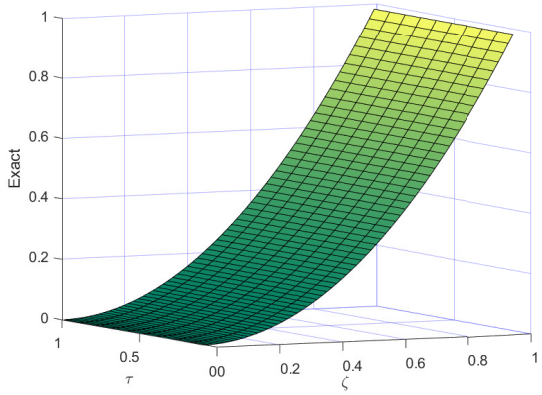

(c) Exact solution at j = 4.

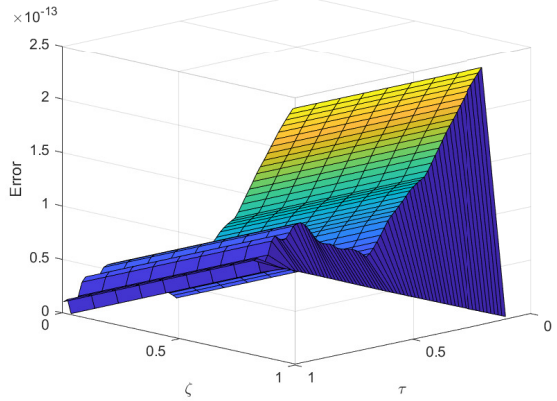

(d) Absolute error at j = 4.

Figure 5: Comparison between approximate solutions and exact solution at different resolution levels.

Problem 5.4. Consider,

$$\frac{\partial^\alpha\mu(\zeta,\tau)}{\partial\tau^\alpha}+\zeta\frac{\partial\mu(\zeta,\tau)}{\partial\zeta}-\frac{\partial^2\mu(\zeta,\tau)}{\partial\zeta^2}=R(\zeta,\tau), \quad 0<\zeta<1, \quad 0<\tau\leqslant 1, \quad 0<\alpha<1,$$

and the IC and BCs are

$$\mu(x,0)=\zeta^2-\zeta^3, \quad \mu(0,\tau)=\mu(1,\tau)=0,$$

where

$$R(\zeta,\tau)=\frac{2\tau^{2-\alpha}}{\Gamma(3-\alpha)}\left(\zeta^2-\zeta^3\right)+\left(\tau^2+1\right)\left(2\zeta^2-3\zeta^3+6\zeta-2\right).$$

The given problem has exact solution as

$$\mu(\zeta,\tau)=\left(\tau^2+1\right)\left(\zeta^2-\zeta^3\right).$$

Table 5: Absolute error of Problem 5.3 at $\alpha = 0.5$, $\tau = 0.5$ with resolution j = 4.

ζ	Haar wavelet [8]	B-Spline Sinc [2]	Chebyshev [31]	Sinc-Legendre [28]	Present method
	m=64	m=20	m=5	m=15	j=6
0.1	1.210E-3	1.369E-09	7.964e-06	6.462e-6	3.5362E-14
0.2	1.259E-3	7.591e-10	3.912e-06	1.578e-5	2.1005E-13
0.3	1.865E-3	1.184e-09	6.162e-06	2.272e-5	5.5344E-14
0.4	7.412E-3	1.068e-09	5.953e-06	2.674e-5	5.1520E-14
0.5	1.000E-6	9.819e-10	2.103e-06	3.004e-4	4.4321E-15
0.6	7.460E-3	1.039e-09	7.639e-06	2.534e-5	3.1104E-14
0.7	1.724E-3	1.031e-09	1.967e-06	2.035e-5	1.1104E-16
0.8	4.990E-3	1.030e-09	8.103e-06	1.320e-5	9.1534E-15
0.9	1.678E-2	1.031e-09	6.019e-06	4.653e-6	6.0192E-14

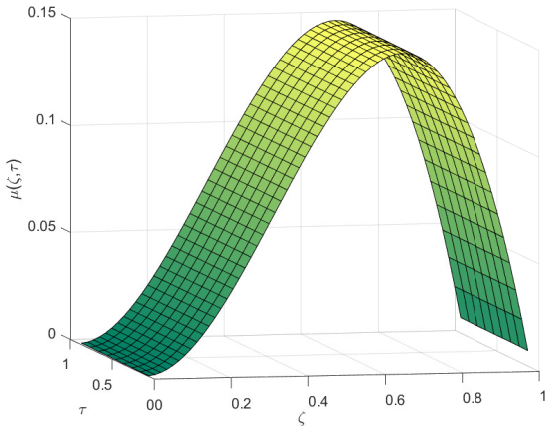

(a) Exact solution at j = 5.

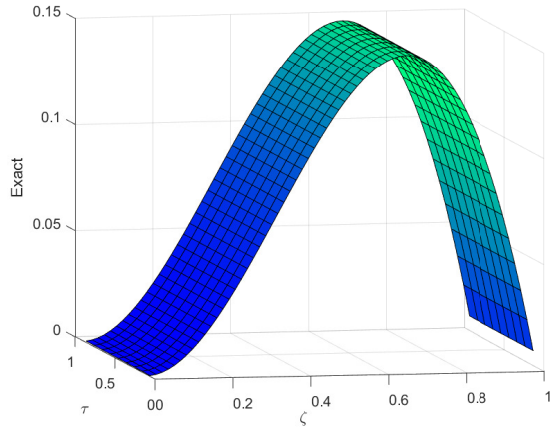

(b) Approximate solutions at j = 5.

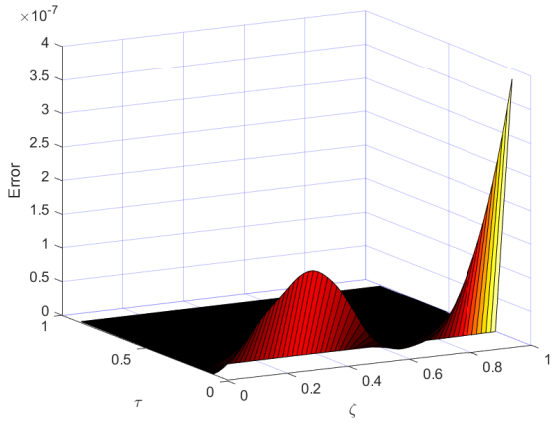

(c) Absolute error at j = 4.

Figure 6: Graphs of approximate and exact solution.

In Figure 6 (a) the approximate solution at resolution levels j = 5 and at $\alpha = 0.05$ (b) the exact solution at resolution levels j = 5 and at $\alpha = 0.05$ (c) shows the absolute error at $\alpha = 0.05$ and $\tau = 0.02$. The time complexity for each numerical examples depends upon the resolution levels, for Problem 5.1 the computation time is 1.511sec at resolution j = 2 and at j = 4 we have 3.237sec, similarly for Problem 5.2 at j = 4 is 3.046 sec and 1.171 sec at j = 2, and for Problem 5.3 the time is 1.123 sec at j = 2 and 3.106 sec

at j = 4. Also for Problem 5.4 the time is 1.401 sec at j = 2 and 3.195 sec at j = 4.

6. Conclusion

In this paper, a generalized Haar wavelet approach is effectively used to find the numerical solution of a TFADEs. The Caputo derivative is utilized in the analysis of fractional derivatives. The approximated solutions of fractional order PDEs subjected to specific BCs were found to match the exact solutions. To demonstrate the efficacy and accuracy of our proposed technique, we present numerical examples and compare them with existing methods such as the Chebyshev collocation method [3, 31], method in [45], Haar wavelet [8], B-Spline [2], and Sinc-Legendre [28]. The graphical representation facilitates a clear observation of how the fractional parameter α evolves over time. Additionally, tables displaying the impact of α on absolute error for a range of values are provided. Analysis of the tables reveals that the error diminishes at an exponential rate, and as the resolution levels j increase, the result converges closer to the exact solution. The 3-dimensional error graph is presented at resolution j = 4. The obtained findings indicate that the suggested method is an excellent tool for numerically solving the TFADEs and can be used to solve other fractional order PDEs. In the future, one can use the proposed method to solve fractional-order nonlinear PDEs, pandemic models, fractional oder integrodifferential equations, and many more.

Acknowledgment

The first two authors are thankful to central university of Haryana for providing necessary facilities to carry out this research. The third author is supported via funding from Prince Sattam bin Abdulaziz University project number (PSAU/2024/R/1445).

References

[1] A. Abbas, A. Khan, T. Abdeljawad, M. Aslam, *Numerical simulation of variable density and magnetohydrodynamics effects on heat generating and dissipating Williamson Sakiadis flow in a porous space: Impact of solar radiation and Joule heating*, Heliyon, **9** (2023), 16 pages. 1

[2] L. Adibmanesha, J. Rashidiniab, *Sinc and B-Spline scaling functions for time fractional convection-diffusion equations*, J. King Saud Univ.-Sci., **33** (2021), 9 pages. 1, 5, 6

[3] M. G. S. AL-Safi, L. Z. Hummady, *Approximate Solution for advection dispersion equation of time Fractional order by using the Chebyshev wavelets-Galerkin Method*, Iraqi J. Sci., **58** (2017), 1493–1502. 4, 6

[4] R. L. Bagley, P. J. Torvik, *A theoretical basis for the application of fractional calculus to viscoelasticity*, J. Rheol., **27** (1983), 201–210. 1

[5] M. Caputo, *Linear models of dissipation whose Q is almost frequency independent. II*, Fract. Calc. Appl. Anal., **11** (2008), 4–14. 1

[6] A. Chang, H. Su, C. Zheng, B. Lu, C. Lu, R. Ma, Y. Zhang, *A time fractional convection-diffusion equation to model gas transport through heterogeneous soil and gas reservoirs*, Phys. A, **502** (2018), 356–369. 1

[7] C. F. Chen, C. H. Hsiao, *Haar wavelet method for solving lumped and distributed parameter systems*, IEE Proc.-Control Theory Appl., **144** (1997), 87–94. 1, 2.3, 4.2

[8] Y. Chen, Y. Wu, Y. Cui, Z. Wang, D. Jin, *Wavelet method for a class of fractional convection diffusion equation with variable coefficients*, J. Comput. Sci., **1** (2010), 146–149. 1, 5, 6

[9] M. Dehghan, S. A. Yousefi, A. Lotfi, *The use of He's variational iteration method for solving the telegraph and fractional telegraph equations*, Int. J. Numer. Methods Biomed. Eng., **27** (2011), 219–231. 1

[10] M. Faheem, A. Khan, A. Raza, *A high resolution Hermite wavelet technique for solving space-time-fractional partial differential equations*, Math. Comput. Simulation, **194** (2022), 588–609. 1

[11] M. M. Izadkhah, J. Saberi-Nadjafi, *Gegenbauer spectral method for time fractional convection-diffusion equations with variable coefficients*, Math. Methods Appl. Sci., **38** (2015), 3183–3194. 1

[12] K. Jothimani, N. Valliammal, S. Alsaeed, K. S. Nisar, C. Ravichandran, *Controllability results of Hilfer fractional derivative through integral contractors*, Qual. Theory Dyn. Syst., **22** (2023), 17 pages. 1

[13] Kamran, M. Irfan, F. M. Alotaibi, S. Haque, N. Mlaiki, K. Shah, *RBF-based local meshless method for fractional diffusion equations*, Fractal Fract., **7** (2023), 1–21. 1

[14] Kamran, R. Kamal, G. Rahmat, K. Shah, *On the Numerical Approximation of Three-Dimensional Time Fractional Convection-Diffusion Equations*, Math. Probl. Eng., **2021** (2021), 16 pages. 1

[15] A. A. Kilbas, H. M. Srivastava, J. J. Trujillo, *Theory and applications of fractional differential equations*, Elsevier Science B.V., Amsterdam, (2004). 2.1, 2.1

[16] S. Khosro, J. T. Machado, I. Masti, *Analysis of dual Bernstein operators in the solution of the fractional convection-diffusion equation arising in underground water pollution*, J. Comput. Appl. Math., **399** (2022), 18 pages. 1

[17] U. Lepik, H. Hein, *Fractional calculus*, In: Haar Wavelets, Mathematical Engineering, Springer, Cham, (2014), 107–122. 1, 2.2

[18] Y. Li, W. Zhao, *Haar wavelet operational matrix of fractional order integration and its applications in solving the fractional order differential equations*, Appl. Math. Comput., **216** (2010), 2276–2285. 4.1

[19] S. G. Mallat, *A theory for multiresolution signal decomposition: the wavelet representation*, IEEE Trans. Pattern Anal. Mach. Intell., **11** (1989), 674–693. 2.2

[20] K. Munusamy, C. Ravichandran, K. S. Nisar, R. Jagatheeshwari, N. Valliammal, *Results on neutral integrodifferential system using Krasnoselskii-Schaefer theorem with initial conditions*, AIP Conf. Proc., **2718** (2023). 1

[21] D. A. Murio, *Implicit finite difference approximation for time fractional diffusion equations*, Comput. Math. Appl., **56** (2008), 1138–1145. 1

[22] K. S. Nisar, S. Alsaeed, K. Kaliraj, C. Ravichandran, W. Albalawi, A.-H. Abdel-Aty, *Existence criteria for fractional differential equations using the topological degree method*, AIMS Math., **8** (2023), 21914–21928. 1

[23] K. S. Nisar, R. Jagatheeshwari, C. Ravichandran, P. Veeresha, *High performance computational method for fractional model of solid tumour invasion*, Ain Shams Eng. J., **14** (2023), 1–11. 1

[24] Z. Odibat, S. Momani, *A generalized differential transform method for linear partial differential equations of fractional order*, Appl. Math. Lett., **21** (2008), 194–199. 1, 1

[25] C. Ravichandran, K. Logeswari, A. Khan, T. Abdeljawad, J. F. Gómez-Aguilar, *An epidemiological model for computer virus with Atangana-Baleanu fractional derivative*, Results Phys., **51** (2023), 1–8. 1

[26] C. Ravichandran, K. Munusamy, K. S. Nisar, N. Valliammal, *Results on neutral partial integrodifferential equations using Monch-Krasnosel'Skii fixed point theorem with nonlocal conditions*, Fractal Fract., **6** (2022), 1–12. 1

[27] D. A. Robinson, *The use of control systems analysis in the neurophysiology of eye movements*, Annu. Rev. Neurosci., **4** (1981), 463–503. 1

[28] A. Saadatmandi, M. Dehghan, M.-R. Azizi, *The sinc-Legendre collocation method for a class of fractional convection-diffusion equations with variable coefficients*, Commun. Nonlinear Sci. Numer. Simul., **17** (2012), 4125–4136. 1, 5, 6

[29] R. Saadeh, *Numerical solutions of fractional convection-diffusion equation using finite difference and finite volume schemes*, J. Math. Comput. Sci, **11** (2021), 7872–7891. 1

[30] S. G. Samko, A. A. Kilbas, O. I. Marichev, *Fractional integrals and derivatives*, Gordon and Breach Science Publishers, Yverdon, (1993).

[31] V. Saw, S. Kumar, *The Chebyshev collocation method for a class of time fractional convection-diffusion equation with variable coefficients*, Math. Methods Appl. Sci., **44** (2021), 6666–6678. 1, 2, 5, 6

[32] F. A. Shah, R. Abass, L. Debnath, *Numerical solution of fractional differential equations using Haar wavelet operational matrix method*, Int. J. Appl. Comput. Math., **3** (2017), 2423–2445. 1, 1, 2.1, 2.2

[33] K. Shah, R. Amin, T. Abdeljawad, *Utilization of Haar wavelet collocation technique for fractal-fractional order problem*, Heliyon, **9** (2023), 1–9. 1

[34] K. Shah, R. Amin, G. Ali, N. Mlaiki, T. Abdeljawad, *Algorithm for the solution of nonlinear variable-order pantograph fractional integro-differential equations using haar method*, Fractals, **30** (2022). 1

[35] F. A. Shah, Kamran, W. Boulila, A. Koubaa, N. Mlaiki, *Numerical Solution of Advection-Diffusion Equation of Fractional Order Using Chebyshev Collocation Method*, Fractal Fract., **7** (2023), 1–20. 1

[36] L. Su, W. Wang, Q. Xu, *Finite difference methods for fractional dispersion equations*, Appl. Math. Comput., **216** (2010), 3329–3334. 1

[37] A. Umer, M. Abbas, M. Shafiq, F. A. Abdullah, M. De la Sen, T. Abdeljawad, *Numerical solutions of Atangana-Baleanu time-fractional advection diffusion equation via an extended cubic B-spline technique*, Alex. Eng. J., **74** (2023), 285–300. 1

[38] K. Wang, *Exact Traveling Wave Solutions for the Local Fractional Kadomtsov-Petviashvili-Benjamin-Bona-Mahony Model by Variational Perspective*, Fractals, **30** (2022), 7 pages. 1

[39] K. Wang, *Solitary wave dynamics of the local fractional Bogoyavlensky-Konopelchenko model*, Fractals, **31** (2023), 9 pages. 1

[40] K.-L. Wang, *New solitary wave solutions of the fractional modified kdv?kadomtsev?petviashvili equation*, Fractals, **31** (2023), 12 pages. 1

[41] J. Xie, *Numerical computation of fractional partial differential equations with variable coefficients utilizing the modified fractional Legendre wavelets and error analysis*, Math. Methods Appl. Sci., **44** (2021), 7150–7164. 1

[42] J. Xie, Q. Huang, X. Yang, *Numerical solution of the one-dimensional fractional convection diffusion equations based on Chebyshev operational matrix*, SpringerPlus, **5** (2016), 1–16. 1

[43] Q. Xu, J. S. Hesthaven, *Discontinuous Galerkin method for fractional convection-diffusion equations*, SIAM J. Math. Anal., **52** (2014), 405–423. 1

[44] L. Zada, I. Aziz, *Numerical solution of fractional partial differential equations via Haar wavelet*, Numer. Methods Partial Differential Equations, **38** (2022), 222–242. 1, 2.1

[45] H. Zhang, F. Liu, P. Zhuang, I. Turner, V. Anh, *Numerical analysis of a new space time variable fractional order advection dispersion equation*, Appl. Math. Comput., **242** (2014), 541–550. 4, 6
[46] J. Zhou, X. Yao, W. Wang, *Two-grid finite element methods for nonlinear time-fractional parabolic equations*, Numer. Algorithms, **90** (2022), 709–730. 1